Effect of Shape Magnetic Anisotropy of Amorphous Fe-B-P Nanoparticles on Permeability

Ji Eun Lee[1], Bulgan Tsedenbal[1], Bon Heun Koo[1] and Seok Hwan Huh[2†]

[1]Department of Materials Science and Engineering, Changwon National University,
Changwon, Gyeongsangnam-do 51140, Republic of Korea
[2]Department of Mechatronics Convergence Engineering, Changwon National University,
Changwon, Gyeongsangnam-do 51140, Republic of Korea

Abstract Many electronic applications require magnetic materials with high permeability and frequency properties. We improve the magnetic permeability of soft magnetic powder by controlling the shape magnetic anisotropy of the powders and through the preparation of amorphous nanoparticles. For this purpose, the effect of the shape magnetic anisotropy of amorphous Fe-B-P nanoparticles is observed through a magnetic field and the frequency characteristics and permeability of these amorphous nanoparticles are observed. These characteristics are investigated by analyzing the composition of particles, crystal structure, microstructure, magnetic properties, and permeability of particles. The composition, crystal structure, and microstructure of the particles are analyzed using inductively coupled plasma optical emission spectrometry, X-ray diffraction, scanning electron microscopy and focused ion beam analysis. The saturation magnetization and permeability are measured using a vibrating sample magnetometer and an LCR meter, respectively. It is confirmed that the shape magnetic anisotropy of the particles influences the permeability. Finally, the permeability and frequency characteristics of the amorphous Fe-B-P nanoparticles are improved.

Key words Fe-B-P, nanoparticles, permeability, soft magnetic materials, shape magnetic anisotropy.

1. Introduction

In the electronics industry and various engineering fields, a material requires high permeability, high saturation magnetization (M_s), low coercivity (H_c), and high resistivity.[1-3] The magnetic factors that determine the permeability and performance at high frequencies are magnetic anisotropy, size distribution, particle surface layers, and the demagnetizing field.[3] Amorphous Fe-B-P particles possess a low coercive field, high saturation magnetization, and high initial magnetic permeability.

Limited research has been conducted on the synthesis and application of amorphous Fe-B-P particles during the last few years. Zhang et al. investigated the particle size, content, and the parameters of amorphous Fe-B-P particles prepared in different solutions under various conditions.[4-7] Shimada et al. developed a chemical process for synthesizing amorphous Fe-B-P submicron particles with magnetic softness that are free from eddy current problems at frequencies a minimum of a few GHz. In that research, particle chains with significantly high permeability were obtained by a chemical reaction in a magnetic field.[2] Yao et al. studied the dynamic permeability comparison of Fe particle composites with different nanoparticles using Ni-Zn ferrite and amorphous Fe-B-P nanoparticles.[3-5]

Although there are many methods proposed to obtain soft magnetic nanoparticles, such as liquid-phase chemical reduction, hydrothermal synthesis, polyol reflux, sol-gel, and co-precipitation, a chemical solution synthesis method was selected that is a simple process and easily imparts the shape magnetic anisotropy.[8-11] Here, we report amorphous Fe-B-P sub-micron chains that are synthesized by a chemical reduction of Fe ions in a magnetic field. In this

work, the main objective is to investigate the magnetization measurements, including observation of the internal structure of the chains by scanning electron microscopy (SEM); further, the permeability of Fe-B-P nanoparticles synthesized without a magnetic field was measured for comparison.

When the particle is amorphous and nano-sized, the specific resistance increases, and the eddy current decreases, thereby improving the frequency characteristics.[12-16] Therefore, the final goal of this study is to prepare amorphous soft magnetic materials with improved initial permeability and frequency characteristics through the shape magnetic anisotropy and synthesis of amorphous nanoparticles.

2. Experimental Procedure

An experimental procedure similar to that described by Zhang et al. was used in this study with few modifications to synthesize Fe-B-P particles by an aqueous reduction method.[4] The reactants were 7.5 g $FeCl_2$, 4.0 g NH_4Cl, 12 g $Na_3C_6H_5O_7$ and 8.0 g NaH_2PO_2, which were dissolved in 50 mL DI water. NaOH solution (2 M) was used to adjust the pH to approximately 9.0. The mixture was stirred at a speed of 120 rpm to obtain a homogeneous solution. Separately, a reduction solution was prepared by using 2 g of $NaBH_4$ in 25 mL of DI water. The reduction solution was then added dropwise (150 mL/h) to the precursor solution. The controlled addition of the reduction solution resulted in the formation of a black-colored precipitate of Fe-B-P particles. To impart the shape magnetic anisotropy of the Fe-B-P particles, a neodymium magnet was attached to the bottom of the beaker during the $NaBH_4$ addition. This action allowed Fe-B-P chains in which particles are connected in a line to become available. The magnetic field of the magnet was approximately 3750 Oe. Precipitated chains of particles were collected with a permanent magnet and washed with DI water and ethanol. Subsequently, the chains were dried at approximately 60 °C in a vacuum oven with a magnet attached to the

bottom of the beaker. In order to observe the effect of the shape magnetic anisotropy, Fe-B-P was also prepared without contributing shape anisotropy by not using a magnet when $NaBH_4$ was added and when the Fe-B-P particles were dried.

Fig. 1 illustrates the preparation process for measuring samples with induced shape magnetic anisotropy. To investigate the effect of the shape magnetic anisotropy of the nanoparticles, a specimen was prepared on an acrylic substrate of toroidal type with an outer diameter of approximately 7 mm, an inner diameter of 3.4 mm, and a height of 2.5 mm. After placing the samples on the acrylic substrate, a magnetic field with an intensity of 2000 Oe was applied on each side using a neodymium magnet. The binder was prepared by mixing PVB, ethyl acetate, toluene, and ethanol, which was then poured into the acrylic substrate, followed by natural drying at room temperature. For comparison, another sample was prepared and mounted on the acrylic substrate through the same route, without the external magnetic field.

The composition of the prepared nanoparticles was measured using an inductively coupled plasma optical emission spectrometry (ICP-OES) (Optima 8300). The crystalline structures of the as-prepared samples were characterized using a BRUKER D8 Advance X-ray diffractometer with Cu Kα radiation of wavelength 1.5406 Å in the angular range of 20 - 80° by scanning at a step size of 0.02°. The surface morphology and particle distribution of the powder samples were observed by field emission scanning electron microscopy (FE-SEM) (MIRA), and the particle size was measured using Image-J software and the magnetic properties were measured at room temperature using a vibrating sample magnetometer (VSM) (Lake Shore 7407). In addition, the permeability of the as-prepared samples was analyzed using an LCR meter (E4991B, Keysight).

3. Results and Discussion

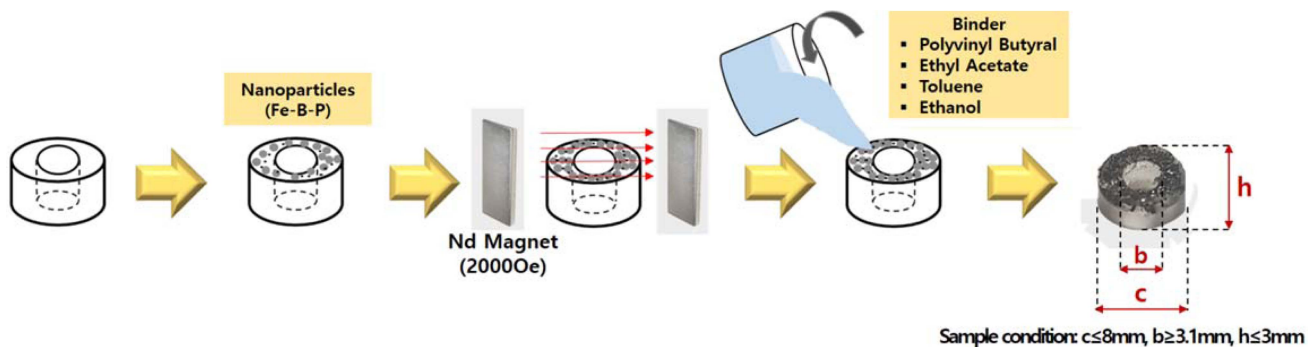Fig. 2 shows the ICP-OES elemental analysis result

Fig. 1. Sample preparation process for measuring induced shape magnetic anisotropy.
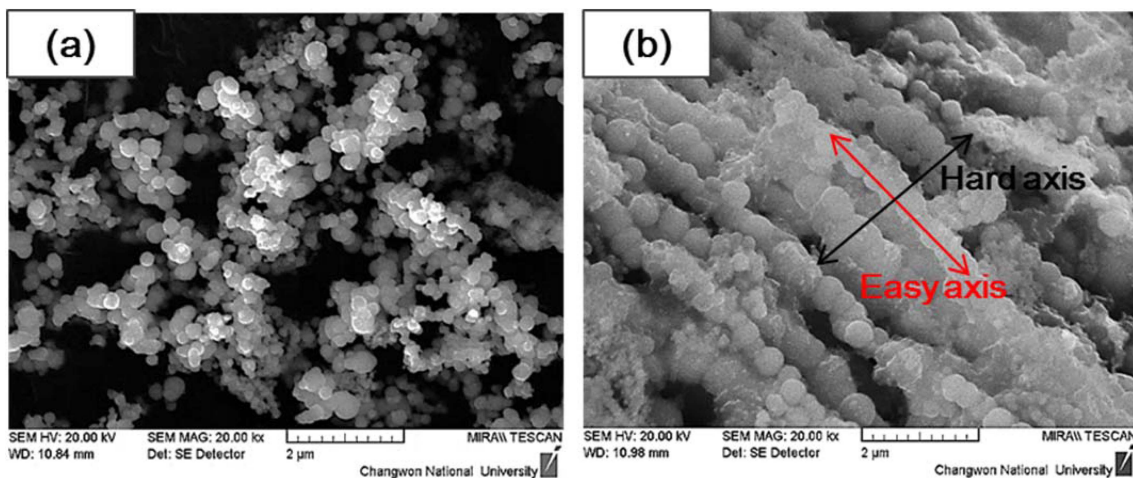
[Fig. 2(a)] and X-ray diffraction (XRD) pattern [Fig. 2(b)] of the as-prepared Fe-B-P particles. The elemental analysis of the compounds confirmed the presence of each element in the nominal compositions of 81.6 %, 7.03 %, and 0.61 % for Fe, boron (B), and phosphorous (P), respectively. The XRD profile of the samples displayed a low intensity and broad diffraction peak at $2\theta = 42°$, which was identified as the main characteristic peak and assigned to the Fe-B-P phase. The comparatively large full width at half maximum (FWHM) and poorly defined intensity of the diffraction peak simply indicate the amorphous nature of the synthesized powder sample. The amorphous nature of the particles was also observed in the FE-SEM images presented in Fig. 3. The sample prepared under the influence of a magnetic field [Fig. 3(b)] in general had a completely different matrix than the powder prepared by removing the external field [Fig. 3(a)]. As seen in Fig. 3(b), the particles were arranged
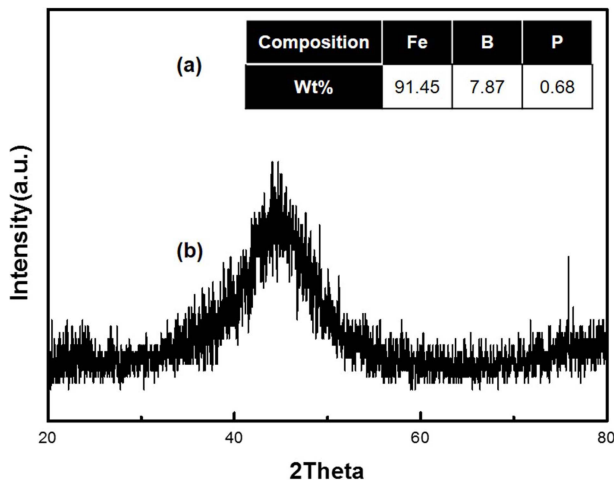
in-line to acquire a pseudo-wire structure, while the particles shown in Fig. 3(a) were randomly positioned. The chain structure of the Fe-B-P particles formed upon application of the magnetic field during the synthesis process because ferromagnetic active Fe-B-P particles tend to respond to the external magnetic field in a parallel direction, and as a result these particles were attracted toward the external field and arranged themselves into long strings of particles. In addition, the absence of any grain boundary and dislocations in the amorphous Fe-B-P particles might have increased the effectiveness of the process and synergistically brought the particles closer in response to the external magnetic field. It can therefore be concluded that the external field induced a shape magnetic anisotropy in the Fe-B-P compound during the synthesis process. The particle affected by the magnetic field has a particle size of about 340 nm [Fig. 3(b)], otherwise, it has a particle size of about 160 nm [Fig. 3(a)]. In the case of the Fe-B-P particle affected by the magnetic field, when it is arranged, the particles do not scatter but agglomerate and promoting growth after nucleation, which is considered to increase the size of the particle. It is thought that further research is needed to clarify the reason for this phenomenon. The impact of the induced shape magnetic anisotropy on the permeability and magnetization of the samples is discussed hereafter.

The shape of the hysteresis loop and saturation magnetization were measured by VSM to confirm the effect of the shape magnetic anisotropy of the Fe-B-P nanoparticles; the results are shown in Fig. 4. For the particles prepared by applying a magnetic field, an easy axis and a hard axis of magnetization were present, and the difference in the slope between the axes was confirmed in the magnetic hysteresis loop. This difference in slope is the effect of the shape magnetic anisotropy, which was formed when particles were arranged in one direction by

Composition	Fe	B	P
Wt%	91.45	7.87	0.68

Fig. 2. (a) Composition of Fe-B-P particles obtained by ICP-OES. (b) XRD pattern of Fe-B-P particles.

Fig. 3. Scanning electron micrographs of Fe-B-P particles prepared (a) without a magnetic field and (b) in a magnetic field at 3750 Oe.

applying a magnetic field, as shown in Fig. 3.

Fig. 5 shows the chain of the Fe-B-P particles prepared by applying a magnetic field at 3750 Oe intensity through focused ion beam (FIB) analysis, in which the particles are seen to be connected and arranged in a line. Moreover, the particles were not simply linked but present in chains, and their central cross section can be seen. The direction formed by the long axis in the chain form is an easy magnetization axis, and the short axis direction perpendicular to it is a hard magnetization axis. In other studies, amorphous nanoparticles with shape magnetic anisotropy grew perpendicular to the major axis direction and deformed their shape, and the length of the particles increased slightly in that direction.[2] Here, FIB analysis revealed that the particles in the indicated area increased in length due to the hard magnetization axis compared to the other particles. In addition, the Fe-B-P particles were not only simply arranged in a line but also
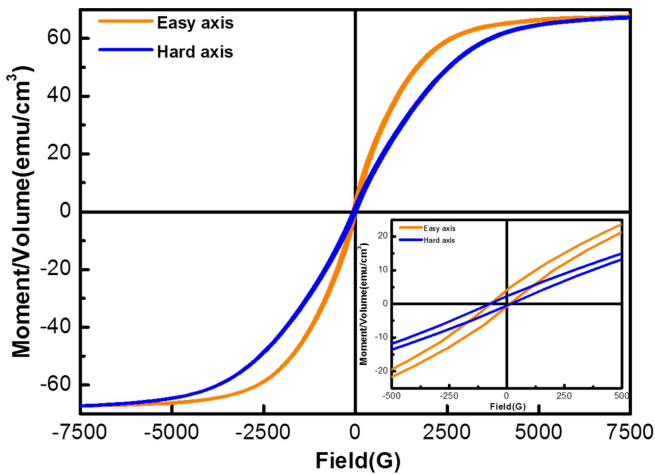
attached to each other during the synthesis process to form a dumbbell-like shape. This is not considered to be physically bound, but that the grain boundaries are interconnected and grown.

The results of the initial permeability due to the existence of the magnetic field in Fig. 6 show that the initial permeability was improved for the particles affected by the magnetic field during the synthesis and drying of the amorphous Fe-B-P nanoparticles. The initial permeability (μ_i) was calculated using the values of the volume fraction of Fe-B-P and the measured permeability through the following equation (Braggeman's equation[6]):

$$q\frac{\mu_i - \mu_e}{\mu_i + 2\mu_e} + (1 - q)\frac{\mu_0 - \mu_e}{\mu_0 + 2\mu_e} = 0 \tag{1}$$

where q, μ_0, and μ_e are the volume fraction of Fe-B-P nanoparticles, permeability of vacuum, and measured permeability of Fe-B-P nanoparticles, respectively.

Table 1 presents the calculated values of permeability and parameters derived from Eq. (1) for the Fe-B-P sample. Comparing the initial permeability of the un-magnetized and magnetized samples, the initial permeability of the magnetized sample increased by approximately 5 times compared with that of the un-magnetized sample, due to the shape of the particles with shape magnetic anisotropy observed in the FIB. According to previous

Fig. 4. Hysteresis loop for Fe-B-P samples measured at an applied field of 0.75 T.
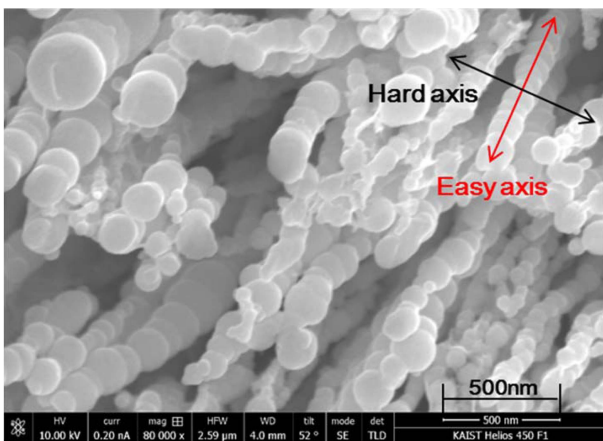
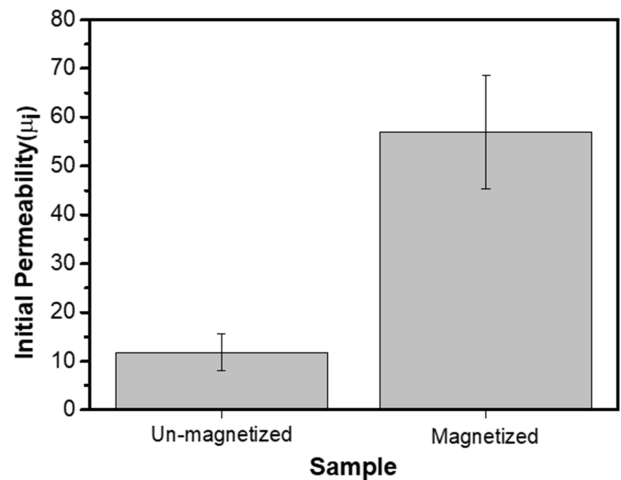**Fig. 5.** Focused ion beam image of the Fe-B-P particles prepared by applying a 3750 Oe magnetic field.

Fig. 6. Initial permeability according to the effect of the magnetic field applied during the preparation of Fe-B-P.

Table 1. Relative permeability and initial permeability according to the intensity of the applied magnetic field during preparation of Fe-B-P.

Magnetic Powders	Saturation Magnetization (M_s)	Volume fraction of powders (%)	μ_e	μ_i
Fe-B-P	23.3	42.5	3.6	11.8
	69.2	37.7	7.8	57.0

research results, when particles exist in a rod form, the permeability is improved by shape magnetic anisotropy.[2] In this study, it was further confirmed that the magnetized sample with the effect of shape magnetic anisotropy has high permeability despite lower volume fraction than the un-magnetized sample. It can be seen that the permeability increases by reducing the demagnetizing field coefficient.

We also investigated the effect of the particle size of Fe-B-P on the frequency characteristics. According to Y. Shimada et al.,[6] the factor that affects the frequency characteristic in which the permeability is maintained up to a specific frequency is eddy current, and the factors that affect the eddy current include particle size, electrical resistance, and frequency. The eddy currents are divided into real [$A(D, \rho, \omega)_{Real}$] and imaginary parts [$jA(D, \rho, \omega)_{Imaginary}$] of permeability. The real part (μ_e, actual permeability) and the imaginary part (μ_e', changed by resistance loss in response to eddy currents) of permeability can be expressed using the following equation.[6] Hence, Eq. (2) allowed us to estimate the frequency response for the samples, the corresponding results for which are shown in Fig. 7. The particle sizes were assumed to be 0.3, 0.5, 3, and 5 μm.

$$\mu_{eddy} = A(D, \rho, \omega)\mu_i, \; k = \sqrt{-\frac{j\omega\mu_i}{2\rho}}$$

$$A(D, \rho, \omega) = 2\frac{kD\cos kD - \sin kD}{\sin kD - kD\cos kD - k^2D^2\sin kD} \quad (2)$$

$$\mu_{eddy} = [A(D, \rho, \omega)_{Real} - jA(D, \rho, \omega)_{Imaginary}]\mu_i$$

$$\omega = 2\pi f\mu_i$$

where μ_{eddy}, μ_i, ρ, and D are permeability when an eddy current occurs, initial permeability, electrical resistivity, and particle size, respectively.

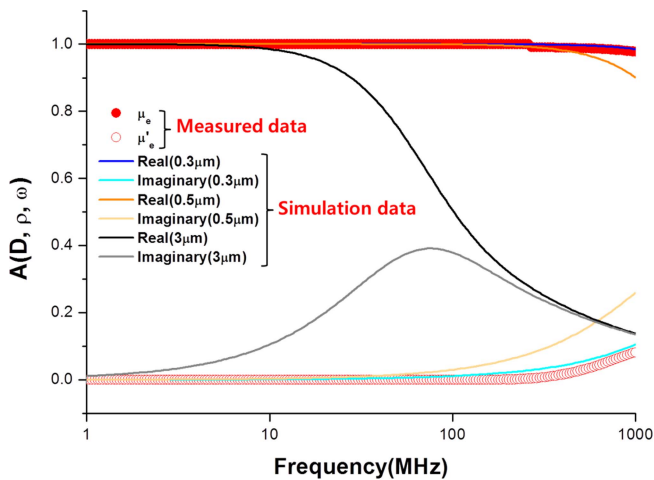The initial permeability (μ_i) and electrical resistivity (ρ)

were fixed at 57 and 1.5×10^4 Ωcm, respectively, and the real and imaginary parts were allowed to change independently with respect to the particle size (D).

As a result of the change in permeability with particle size, the smaller the particle size, the less eddy current loss occurred in the high frequency band, which means that the permeability was maintained up to a high frequency. Among the results of permeability according to particle size, when the particle size was 5 μm, the resistance loss due to eddy current increased the most rapidly, and the real part of the permeability decreased significantly as the frequency increased. In particular, after approximately 50 MHz, the permeability decreased extremely rapidly compared with the trends in particle sizes of 0.3 μm and 0.5 μm. As the operating frequency increased, the permeability decreased with increasing frequency, resulting in eddy current losses and permeability losses.

The real and imaginary parts of the actual permeability measured were most similar to the data for the particle size of 0.3 μm, which can be used to predict the particle size. The prepared Fe-B-P particles were formed in a long chain, thus improving the permeability, and in frequency characteristics, each particle was recognized as a single particle, exhibiting a frequency characteristic with a fine particle size. As can be seen from the scale bar of the FE-SEM image shown in Fig. 3, it was confirmed that the actual prepared Fe-B-P particle had a particle size of approximately 0.3 μm. In addition to the effect of shape magnetic anisotropy, the amorphous nanoparticles possessed a small particle size and a large electrical resistivity, such that the eddy current loss was not large. Thus, when an eddy current occurred, the decrease in permeability was small.

Therefore, amorphous Fe-B-P nanoparticles with shape magnetic anisotropy can be used in a high frequency band, and the frequency characteristics can be improved through a small particle size and high electrical resistance along with an improvement in permeability due to a decrease in the demagnetizing field coefficient.

4. Conclusions

We have conducted research on the development of high-permeability magnetic materials using soft magnetic particles through the control of the shape magnetic anisotropy of the particles and the production of amorphous nano-particles. Fe-B-P nanoparticles in a chain-like form were prepared by connecting spherical particles with a particle size of approximately 300 nm using a magnet. Through the preparation of these chain nanoparticles, high-permeability nanoparticles with shape magnetic anisotropy and a reduced demagnetizing field coefficient were obtained, and the

Fig. 7. Relative permeability of Fe-B-P predicted by particle size.

initial permeability was improved by a factor of five compared to the particles without shape magnetic anisotropy. In addition, the eddy current loss was reduced by the amorphous Fe-B-P nanoparticles exhibiting high electrical resistivity and small particle size, and their frequency characteristics were improved. This research demonstrates that a simple chemical method can be used to produce materials with the desired characteristics of high permeability and electrical resistivity for electronic and engineering applications.

Acknowledgment

References

1. C. Yao, Y. H. Zhang, J. Chen, D. X. Bao, S. Li and G. W. Qin, Mater. Res. Innovations, **18**, S4-634 (2014).
2. Y. Shimada. Y. Endo, M. Yamaguchi, S. Okamoto and O. Kitakami, IEEE Trans. Magn., **47**, 2831 (2011).
3. C. Yao, Y. Shimada, G. W. Qin, W. L. Pei, S. Okamoto, O. Kitakami, Y. Endo and M. Yamaguchi, IEEE Trans. Magn., **47**, 3160 (2011).
4. Y. Zhang, X. Wang, C. Yao and G. Qin, Mater. Sci. Forum, **848**, 652 (2016).
5. Y. Zhang, C. Yao, Y. Chao and G. Qin, Hyperfine Interact., **219**, 101 (2013).
6. Y. Shimada, Y. Endo, M. Yamaguchi, S. Okamoto and O. Kitakami, J. Magn. Soc. Jpn., **33**, 95 (2009).
7. J. Ding, Y. Li, L. F. Chen, C. R. Deng, Y. Shi, Y. S. Chow and T. B. Gang, J. Alloys Compd., **314**, 262 (2001).
8. N. J. Tang, W. Zhong, H. Y. Jiang, Z. D. Han, W. Q. Zou and Y. W. Du, Solid State Commun., **132**, 71 (2004).
9. P. M. Paulus, F. Luis, M. Kröll, G. Schmid and L. J. D. Jongh, J. Magn. Magn. Mater., **224**, 180 (2001).
10. D. Lin, P. Zhou, W. N. Fu, Z. Badics and Z. J. Cendes, IEEE Trans. Magn., **40**, 1318 (2004).
11. J. Shen, B. Gao, H. W. Zhang, F. X. Hu, Y. X. Li, J. R. Sun and B. G. Shen, Appl. Phys. Lett., **91**, 142504 (2007).
12. H. Su, H. Zhang, X. Tang and X. Xiang, J. Magn. Magn. Mater., **283**, 157 (2004).
13. O. Acher, S. Queste, M. Ledieu, K.-U. Barholz and R. Mattheis, Phys. Rev. B: Condens. Matter Mater. Phys., **68**, 184414 (2003).
14. L. Sun, P. C. Searson and C. L. Chien, Appl. Phys. Lett., **79**, 4429 (2001).
15. J. Cui, T. W. Shield and R. D. James, Acta Mater., **52**, 35 (2004).
16. Y. Shimada, Y. Endo, M. Yamaguchi, S. Okamoto, O. Kitakami, Y. Imano, H. Matsumoto and S. Yoshida, IEEE Trans. Magn., **45**, 4298 (2009).

Author Information

Ji Eun Lee
창원대학교 신소재공학부 석사후연구원

Bulgan Tsedenbal
창원대학교 산업기술연구원 박사후연구원

Bon Heun Koo
창원대학교 신소재공학부 교수

Seok Hwan Huh
창원대학교 메카융합공학과 교수